

Study and Analysis of Below Knee Osseointegration Prosthesis

Saif M. Abbas^{1*} , Jumaa S. Chiad² , Ayad M. Takhakh³ 

¹Prosthetic and Orthotic Engineering Department, College of Engineering, Al-Nahrain University, Baghdad, Iraq

^{2,3}Mechanical Engineering Department, College of Engineering, Al-Nahrain University, Baghdad, Iraq

*Email: saif.mohammed@nahrainuniv.edu.iq

Article Info	Abstract
<p>Received 18/04/2024</p> <p>Revised 23/05/2024</p> <p>Accepted 24/05/2024</p>	<p>Osseointegration is a medical metal implant into the residual bone of an amputated limb. The prosthesis can be connected to this implant. Different prosthetic components were thoroughly assessed using experimental testing and simulation results. The prosthetic foot's outstanding mechanical qualities were revealed during tensile testing on carbon and glass fiber composite materials. The mechanical properties of these materials yield stress $\sigma_y = 70\text{MPa}$, ultimate tensile strength $\sigma_{ult} = 162\text{MPa}$, and Young's modulus $= 2\text{GPa}$. For osseointegrated prosthetic components, the implant material yield stress $\sigma_y = 470\text{MPa}$, ultimate tensile strength $\sigma_{ult} = 558\text{MPa}$, and Young's modulus $= 2.7\text{GPa}$, Ti-13Nb-13Zr alloy demonstrated excellent tensile and compression capabilities. Important information on both metallic and composite materials' durability under cyclic loads was obtained via fatigue testing. The numerical simulations were carried out utilizing the ANSYS 17.2 program. The analysis shows that the safety factor for a prosthetic model with below-knee osseointegration is 1.563. So that the Von-Mises stress and total deformation were acceptable. Integrating actual data, such as the results of tensile, compression, and fatigue tests, with numerical simulations highlights the significance of materials and mechanical analysis in developing prosthetic technology, promising improved mobility and quality of life for amputees.</p>

Keywords: Composite material; Osseointegration; Prosthetic Foot; Prosthetic model; Simulation (Ansys).

1. Introduction.

A metal implant is surgically attached directly to the residual bone of an amputated limb in osseointegrated lower limb prostheses, sometimes referred to as bone-anchored prostheses. A tiny stoma is inserted through the skin to bind the external prosthesis to this implant, which acts as a stable connecting point. This method can offer more stability and a more natural sensation than conventional socket-based prostheses [1],[2]. The effective integration of implants into the bone for various uses is how medical therapy has significantly improved due to osseointegration [3]. In prosthetics, osseointegration attaches a prosthetic component to an implant firmly and with a stronger connection to the body of patients who have amputated limbs to improve their quality of life and comfort [4]. Patients who wear socket prosthetics experience pain due to sweating, skin irritation, allergy problems, and lack of body suspension. Osseointegration implants are results for these problems, which are used for transfemoral amputations due to trauma or malignancy [5].

Assessing the full potential of osseointegration to enhance the lives of amputees will depend heavily on this continuing research [6],[7]. The surgical attachment of a threaded titanium implant to the remaining bone during the initial procedure to directly anchor a prosthetic limb to the humeral bone. In the subsequent procedure, an abutment (a titanium extension) is fitted into the fixture and fastened with an abutment screw. The prosthetic limb's connection point is the abutment, which pokes through the skin [8]-[10]. Due to worries about infection, the notion of a bone-anchored implant piercing the skin and coming into touch with the outside environment is problematic. Although potentially dangerous germs can colonize the skin penetration site, few infections requiring implant removal have ever happened. This indicates that, despite the initial reservations, this approach has shown the potential to prevent infections and enable prosthetic limbs to work [11]. Transfemoral amputees have been using the Osseointegrated Prostheses for the Rehabilitation of Amputees (OPRA) implant system, created by Integrum AB in Sweden, with success for more than 20 years. At the 2-year follow-up point, recent

prospective research comprising 51 patients found a cumulative success rate of 92% [12]. Compared to conventional socket prostheses, patients who received the OPRA implant system reported greater hip range of motion (ROM) and enhanced sitting comfort. In transfemoral amputees, radio stereometric analysis also showed stable implant fixation and periprosthetic bone remodeling, which is comparable to what is seen around uncemented hip stems. These results demonstrate how osseointegration helps transfemoral amputees live better lives and operate more normally [13]-[15]. The applications of osseointegrated prostheses are increasingly observed in situations of traumatic amputations and malignancies; however, the indications are still being developed. It's crucial to remember that there are certain limitations to this method [16]-[18]. Osseointegrated prostheses are typically not advised for skeletally immature patients, elderly patients over the age of 70, people with diabetes, people with peripheral vascular disease, women who are pregnant, people who are undergoing chemotherapy, people who are taking immunosuppressive medications, people who have psychiatric conditions, and people who have trouble adhering to treatment regimens. The benefits of the osseointegrated prosthesis can be substantial for qualified applicants despite these contraindications. These benefits can include a higher quality of life, a wider range of motion in the hip joint, greater sitting comfort, the capacity to feel sensations through prosthesis (osseoperception), better walking ability, and the autonomy to put on and take off prosthesis [19]-[25]. This study aimed to assess the mechanical characteristics of the implant, leg, and foot and analysis for below-knee prosthetics with an osseointegration model using Ansys.

2. Experimental Procedures.

The study is centered on manufacturing and examining samples for below-knee prosthetic components such as osseointegration implants, pylons, and feet using specific materials and specialized equipment and analyzing the patient's gait cycle.

2.1. Material Selection for the implant.

Samples of the Ti-13Nb-13Zr ASTM F-1713:2008 [26] alloy was provided for the experiments in cylindrical sections with a 13 mm diameter and 400 mm length. From the Baoji, China-based Shaanxi Yuzhong Industry Development Co. These samples were used to establish standardized specimens for mechanical testing, especially to ascertain tensile, compressive, and fatigue characteristics. The Wire Electrical Discharge Machining process was used to get the necessary geometries. Prefabricated rods of decreased size were manufactured and modified to the required specifications using a CNC lathe ST-10 and a CNC milling machine VF-1 from Oxnard, California-based Haas Automation Inc. The chemical makeup of the Ti-13Zr-13Nb alloy employed in the study is shown in Table 1 to completely describe the examined alloy and demonstrate its usefulness as an implantation material. The Ministry of Science and Technology in Baghdad, Iraq, has X-Ray Fluorescent (XRF) testing used for the chemical analysis.

Table 1. Chemical Composition (wt%) of Ti-13Zr-13Nb Base Alloy.

Elements	wt. pct. %	wt. pct. % [26]
Zr	15.22	12.5 - 14 ± 0.40
Nb	13.45	12.5 - 14 ± 0.40
Fe	0.1155	0.11 ± 0.10
Mo	0.077	0.051 ± 0.02
Zn	0.0527	0.0871 ± 0.02
Mn	0.0387	0.0322 ± 0.1
Cu	0.0432	0.08 ± 0.02
Ti	69.94	70.46 - 77.46
Residual Element	0.13503	
Sum of Concentration	99	

2.2. Material of the pylon and foot

2.2.1. Carbon and Glass Fibers.

Combining glass and carbon fibers to create composite materials gives them outstanding strength, lightweight, and stiffness. These materials are frequently utilized to strengthen and improve the prosthetic pylon and foot, increasing their endurance and resilience to wear and strain by normal use and walking.

2.2.2. Resin combined with a hardener at a ratio of 80:20.

This investigation employed a polymer resin, especially an 80:20 PMMA resin combination. The carbon and glass fibers are impregnated with this resin-hardener mixture to provide a strong and stiff composite framework for the prosthetic pylon and foot.

2.3. Tools and devices

2.3.1 A mould from Jepson

The test specimens of hybrid composite material for the pylon and foot are shaped and molded using a 3 * 6 * 28 cm Jepson mold.

2.3.2 Pressure vacuum

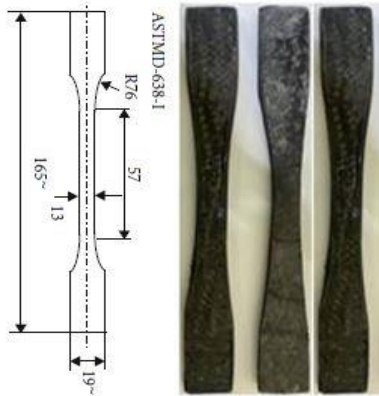
A pressure vacuum system, more precisely, the Vacuum pump Vac M1.5, is used during the production process to guarantee no gaps between the resin and fiber layers. This technique aids in achieving adequate impregnation and material bonding.

2.3.3 Tensile Test Device

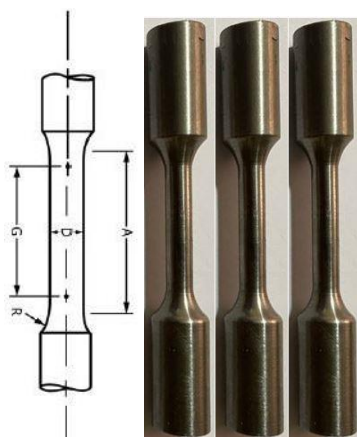
The tensile test instrument assesses the mechanical properties and tensile strength of the materials used to construct prosthetic feet, pylons, and implants. This instrument is essential for determining the material's durability and ability to withstand stretching forces.

Three samples were tested and assessed in accordance with ASTM D638 Type I [27] standards for composite materials. As shown in Fig. 1, these samples were created using various lay-

up arrangements that produced a consistent thickness of 6.7mm. Three samples were made and tested in line with ASTM E8/E8M-16a [28] standards, which are normally applied to metallic materials. This meticulous testing methodology aids in evaluating the functionality and characteristics of composite and metallic parts utilized in prosthetic feet, pylons, and implants.



(a)



(b)

Figure 1. Tensile test specimen and dimension (a) for composite material (b) for metallic material

2.3.4 Fatigue test for a flat specimen

As shown in Fig.2, the fatigue test evaluates the fatigue life and sturdiness of the composite material used in the prosthetic pylon and foot. This test is essential for determining how well the material can survive repeated cycles of stress and strain over time, which is significant for prosthetic components that are used continuously.

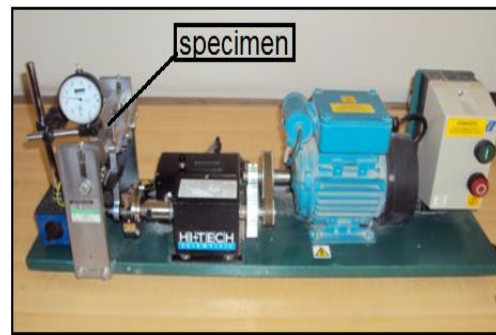


Figure 2. Fatigue test.

According to ASTM D3479[29] specifications, flat specimens of the same composite material measuring 100mm in length and 10mm in breadth are repeatedly loaded. As shown in Fig. 3, these samples have been painstakingly prepared to match the fatigue testing device's necessary size and technical requirements. The thorough testing process makes this exact evaluation of the material's performance characteristics and fatigue behavior possible.

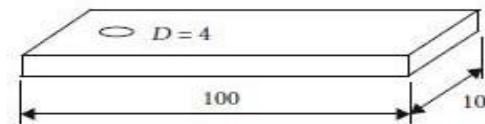


Figure 3. Fatigue specimen and dimension for composite materials

2.4 Cases Study

The patient in Fig. 4 with the osseointegration prosthesis exhibited the following traits: 30 years old, male, 1.60 m tall, and 74 kg in weight. The left sides were amputated. The patient participated in this study after giving their informed consent in accordance with the ethical approval obtained from Al-Nahrain University's College of Engineering. Experiments were performed on a wooden boardwalk with a force plate. In Baghdad, Iraq, AL Nahrain University offered the examination.



Figure 4. Cases Study

3. Numerical Analysis of Osseointegration Prosthesis

3.1 Bringing the SOLIDWORKS Model

The initial stage is importing the prosthetic's 3D model from SOLIDWORKS into ANSYS Workbench, as shown in Fig. 5. This connection allows for additional analysis and simulation of the prosthesis within the ANSYS environment.

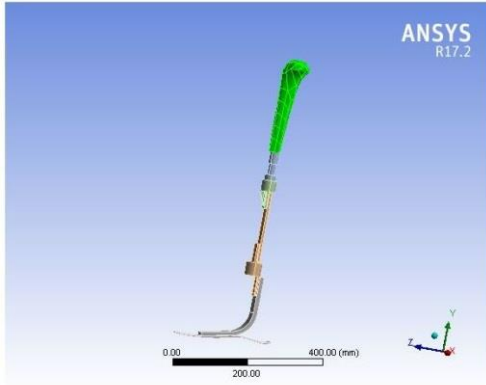


Figure 5. Solid Works Model

3.2 Apply Material Characteristics

Next, specify in ANSYS the material properties of each prosthesis component. This involves defining characteristics that appropriately depict how each material responds to various loading circumstances, such as density, Poisson's ratio, Young's modulus, and others. These material characteristics must be defined correctly for appropriate modeling and performance analysis of the prosthesis.

3.3 Mesh Generation

The model will then be discretized by adding a mesh to its surfaces. The model is divided into finite elements during the meshing process, which ANSYS may employ for analysis. A high-quality mesh must be created to get accurate results. As seen in Fig. 6, ANSYS Workbench offers a variety of meshing controls and choices to help users achieve the required mesh density and choose the right element types. The meshing of the prosthetic model utilized ten-node tetrahedral elements. In this instance, it has 11989 nodes and 6171 components, necessary for accurate simulations and analysis.

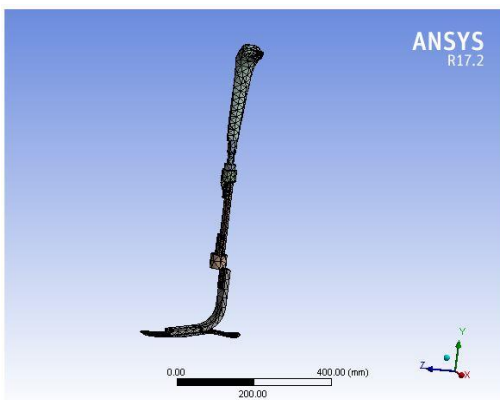


Figure 6. Mesh Generation

3.4 Boundary Conditions

The boundary conditions resemble actual situations where the prosthetic foot will be used. The ground reaction force under the foot for three scenarios at the heel, mid, and toe-off of the foot and fixed support at the top of the head of the tibia, as shown in Fig. 7, was applied. These boundary conditions aid in simulating the prosthetic foot's actual mechanical behavior while performing various tasks.

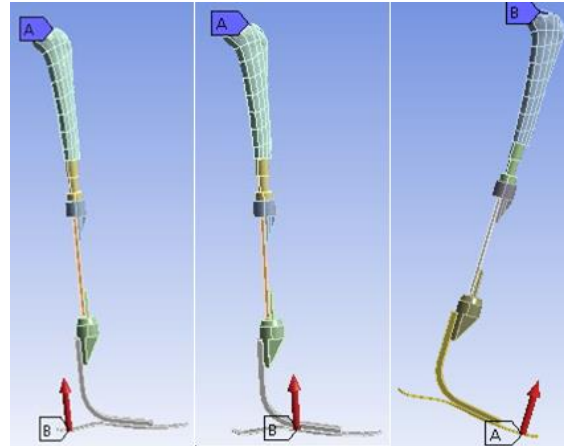


Figure 7. Boundary Conditions for three scenarios.

3.5 Determine the sort of analysis

Select the analysis type that best supports your unique goals. Common analyses for prostheses models depend on the desired function of the prosthesis and include the following:

Analyzing the prosthesis' responses to static loads and forces using the static structural method helps one comprehend how it behaves when standing or walking normally.

Fatigue Analysis: Fatigue analysis is crucial for assessing the robustness and fatigue life of the prosthesis under cyclic loading circumstances, such as activities requiring repetitive motions like walking or running.

The right analysis type must be chosen to achieve individual objectives and provide a thorough assessment of the prosthetic's performance.

Table 2 displays the mechanical characteristics of cortical bone.

Table 2. Mechanical properties of the cortical bone [29]

Sample	σ_y (MPa)	σ_{ult} (MPa)	E (GPa)
Cortical bone	175	205	20

4. Results and Discussion

4.1. Tensile Properties Results for Composite Material

This test shows that the prosthetic foot's composite materials persevered a tensile test, producing the stress-strain curves shown in Fig. 8. These curves were used to compute key mechanical characteristics, which are displayed in Table 3 and include Young's modulus (E), yield stress (y), and ultimate tensile strength (ult).

The combination of glass and carbon fibers gives the composite material high yield stress, ultimate tensile strength, and elastic modulus. These fibers are well known for their exceptional tensile properties, which allow them to withstand high tensile strains without cracking or undergoing considerable deformation. This property helps explain why the composite material's yield stress and high elastic modulus exist.

Table 3. The results of the tensile test were evaluated from stress-strain curves.

Sample	σ_y (MPa)	σ_{ult} (MPa)	E (GPa)
1	69	163.367	1.95
2	71	160.07	2.17
3	68.2	164.7	1.98

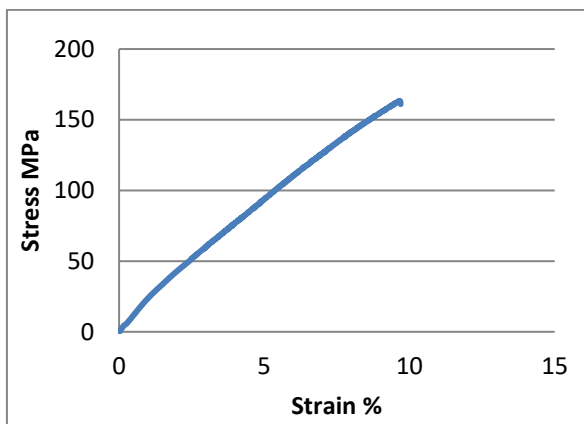


Figure 8. Average stress-strain curve for foot and leg.

4.2. Tensile Properties Results for Ti-13Nb-13Zr Alloy.

When stress is measured at the location where 0.2% plastic deformation occurs, the mechanical characteristics found in this work show curves with a distinctive shape typical for materials with proof stress. During the static tensile testing, the ASTM standard specifications were established for the evaluated Ti-13Nb-13Zr alloy samples. The average yield strength (YS) at 0.2% elongation was 483MPa, the average ultimate tensile strength (UTS) was 552.843 MPa, and the average elongation (A) was 19.66%. Young's modulus, another crucial factor in biomedical engineering, was 143 GPa, as seen in Fig. 9. A summary of these findings is shown in Table 4, along with comparisons to the ASTM F1713 [26] requirements and the supplier's certificate, which are critical for determining if the material is appropriate for prosthetic applications in biomedical engineering.

Table 4. Mechanical properties of Ti-13Nb-13Zr alloy.

Sample	σ_y (MPa)	σ_{ult} (MPa)	E (GPa)[30]
1	471.558	558.492	143
2	507.103	543.638	143
3	470.235	556.4	143

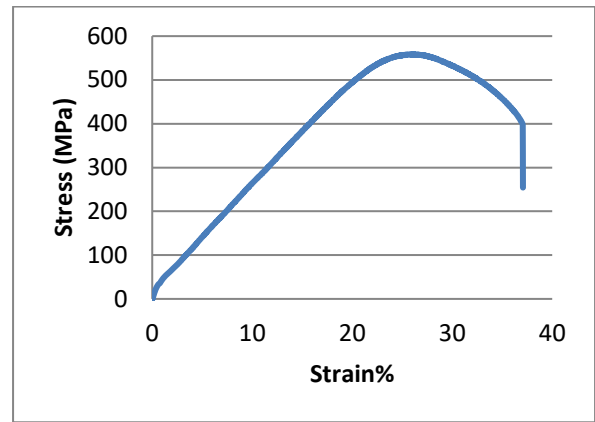


Figure 9. Average stress-strain curve for implant material.

The findings achieved closely match the manufacturer's requirements. Any variances can be ascribed to variations in the research techniques used. Additionally, the supplier's certificate lacked data that matched the outcomes of static compression and bending tests. It's important to note that changes in the requirements compared to the ASTM F1713 [26] standard and the findings of this study most likely resulted from the supplier's annealing process, which deviated from the description in the standard. The stress-strain curves for the examined alloy from compression and tensile testing. When reviewing these figures, it becomes clear that the curves have the typical form of materials without a clear yield point. All static tensile test samples' produced curves showed linear properties within the bounds of Hooke's law, enabling the calculation of Young's modulus.

4.3. Fatigue Property Results for Composite Material

The room-temperature fatigue tests on the carbon-glass fiber laminations used in this work are useful for evaluating the material's performance under repeated cycle loads. Fatigue failure is a major worry in many engineering applications, including prosthetic feet, as it impacts a material's capacity to withstand repeated stress cycles over time. The data obtained establishes the link between fatigue failure stress and cycle count.

Fig. 10 illustrates the observed inverse connection between fatigue failure stress and the number of cycles to failure. When the fatigue failure stress drops, the material may take more cycles before failing (as stated by the equation with $C = -0.158$ and $N = 79.16$). Higher fatigue failure stresses, on the other hand, suggest that the material will break after fewer loading cycles.

The results of fatigue testing are vital in ensuring that prosthetic feet for people who have had their lower limbs amputated are appropriate for long-term usage and can resist the rigors of everyday activity. This information is essential for improving the robustness and dependability of prosthetic components.

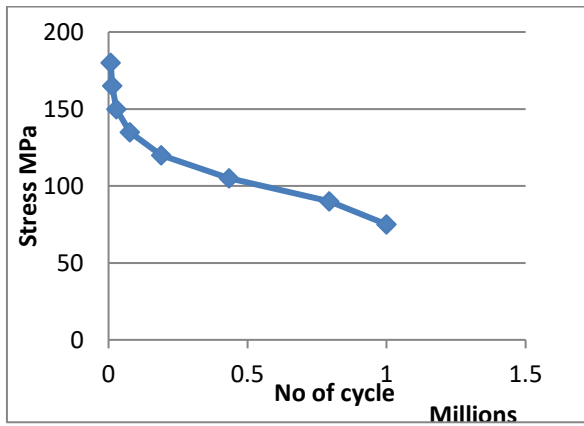


Figure 10. S-N curve for carbon-glass fiber

As the number of cycles to failure rises, the fatigue strength of the Ti-13Nb-13Zr implant samples constantly decreases, as shown in Fig. 11 [32].

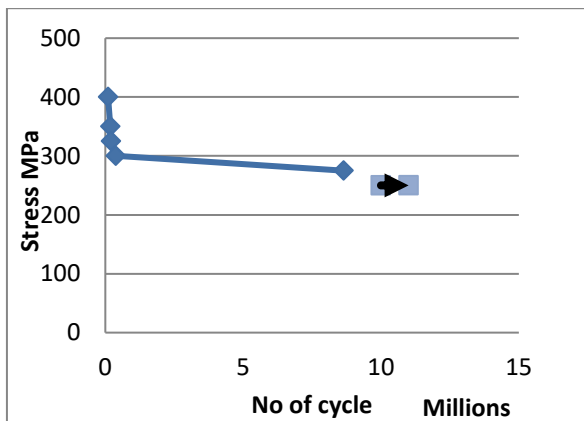


Figure 11. S-N curve for 13Nb-13Zr implant [32]

4.4. Force Plate Results.

Using the force plate to determine the ground reaction forces applied on an implant's abutment at heel contact, mid-stance, and toe-off during the gait cycle. It's crucial to note any significant differences between the traits of the right and left legs.

By examining the peak values of forces and moments during heel contact and toe-off, clinicians and researchers may thoroughly analyze the loading conditions on the implant's abutment and gauge the implant's functioning and stability throughout the gait cycle.

Fig. 12 shows the force curve over time for the left and right legs, represented by the red and green lines. The maximal force recorded is 600 N, providing a visual picture of the dynamic stress that the implant underwent across various gait cycle phases.

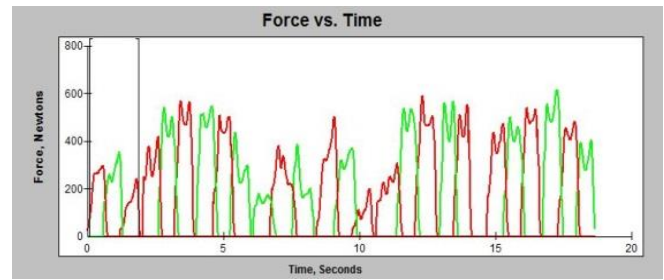


Figure 12. Force vs. Time.

4.5. ANSYS Results

Analysis of a prosthetic model using the ANSYS Workbench software (version 17.2) is a standard procedure in biomechanical engineering to determine total deformation, equivalent stress (Von Mises), and safety factors. Fig. 13 displays the safety factors derived from the numerical analysis results for the prosthesis model. According to the study, most prosthetics are located in the blue and green zones, where the safety factor is greater than 5, which is substantially higher than the necessary value of 1.25. A small portion on the lower side of the prosthetic model has a safety factor of less than 5. The safety factors, total deformation, and equivalent stress for three scenarios for the below knee osseointegration model, obtained from the numerical analysis results, are shown in Table 5.

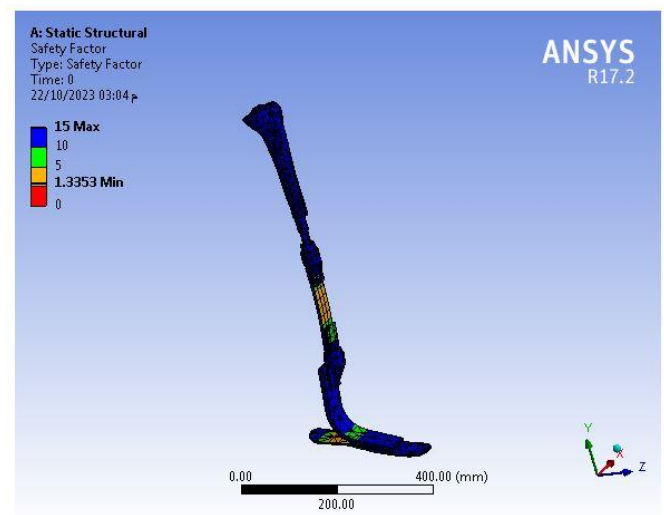


Figure 13. Fatigue factor of safety at heel.

Fig. 14 displays The maximum Von-Mises stress for the prosthetic model, which shows a stress distribution of about (116.23MPa) which is less than when compared to the yield stress (470 MPa and 70 MPa for the implant material, leg, and foot, respectively); it can be said that the static design is satisfactory for the static design had generally acceptable total deformations, low Von-Mises stress, and suitable safety factors.

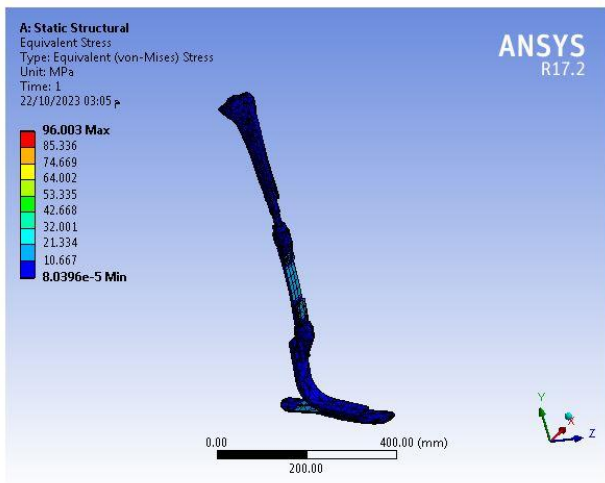


Figure 14. Equivalent stress (von Mises) at heel.

Fig. 15. shows the prosthetic model's overall distortion. The overall deformation study shows that the maximum deformations (10mm) are suitable for prosthetic model applications.

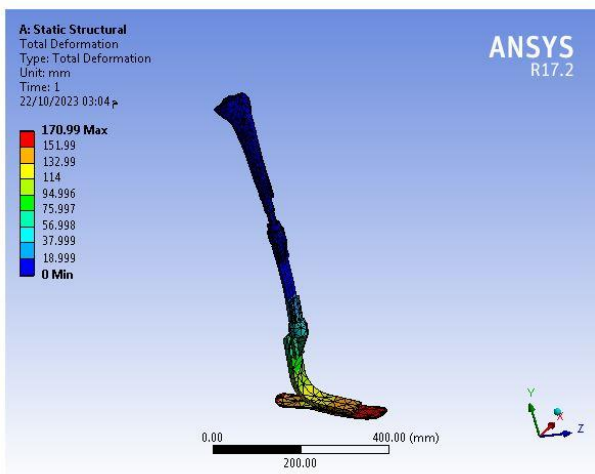


Figure 15. Total deformation at heel.

Table 5. FEM Analysis Results

Applied force (N)	Total deformation (mm)	Equivalent stress (Mpa)	Safety factor
heel	170.7	96.003	1.335
Midfoot	221.06	116.23	1.013
metatarsal	61.51	84.858	1.015

5. Conclusions

The research and examination of below-knee osseointegration prostheses represents a notable development in prosthetic limb technology. ANSYS Workbench 17.2 was used for the finite element analysis, mechanical testing, and other areas of this thorough examination.

Both composite (carbon-glass fiber) and metallic (Ti-13Nb-13Zr alloy) materials had their tensile characteristics assessed. The composite materials were ideal for prosthetic components because they had high yield stress, ultimate tensile strength, and Young's modulus. Fatigue tests were performed on both metallic and composite components. Determining the materials' long-term durability requires knowing how they react to cyclic loading conditions, and this data was informative. The maximum Von-Mises stress for the prosthetic model shows a stress distribution of about (116.23MPa) which is less than when compared to the yield stress (470 MPa and 70 MPa for the implant material, leg, and foot, respectively); it can be said that the static design is satisfactory for the static design had generally acceptable total deformations, low Von-Mises stress, and suitable safety factors.

Funding No external funding.

Conflict of Interest: The authors declare no conflict of interest.

Author Contribution Statement Author Saif M. Abbas suggested the problem of the research, developed the foot prosthetic, and conducted the experimental work and analysis of the design of the prosthetic model using ANSYS 17.2.

Authors Jumaa S. Chiad and Ayad M. Takhakh verified the analytical methods, conducted the manuscript's structure, and organized the outcomes of this study.

The template is used to format your paper and style the text. All margins, line spaces, and text fonts are prescribed; please do not alter them.

References

- [1]. J. Hoellwarth, K. Tetsworth, R. Rozbruch, B. Handal, A. Coughlan, and M. Al Muderis, "Osseointegration for Amputees: Current Implants, Techniques, and Future Directions," *JBJS. Rev.* vol.8. no.3, pp 0043, 2020. <https://doi.org/10.2106/jbjs.rvw.19.00043>
- [2]. S.M., Abbas, K.K., Resan, A.K. Muhammad, and M., Al-Waily, "Mechanical and fatigue behaviors of prosthetic for partial foot amputation with various composite materials types effect". *International Journal of Mechanical Engineering and Technology*, vol. 9, no. 9, pp.383-394. 2018. https://iaeme.com/MasterAdmin/Journal_uploads/IJMET/VOLUME_9_ISSUE_9/IJMET_09_09_042.pdf
- [3]. P. Branemark, B. Hansson, R. Adell, U. Breine, J. Lindstrom, and O. Hallen, "A 15-Year Study of Osseointegrated Implants in the Treatment of the Edentulous Jaw," *Scand J Plast Reconstr Surg Suppl*, vol.16, pp. 1-132, 2020. [https://doi.org/10.1016/s0300-9785\(81\)80077-4](https://doi.org/10.1016/s0300-9785(81)80077-4).
- [4]. Y. Li, and L. Fellander-Tsai, "The bone anchored prostheses for amputee's historical development, current status, and future aspects," *Biomaterials*, vol. 273, pp. 120836, 2021. <https://doi.org/10.1016/j.biomaterials.2021.120836>
- [5]. R. Leijendekkers *et al.*, "Comparison of bone-anchored prostheses and socket prostheses for patients with a lower extremity amputation: a systematic review," *Disabil Rehabil*; vol. 39, pp. 1045-1058, 2017. <https://doi.org/10.1080/09638288.2016.1186752>
- [6]. P. Frolke, R. Leijendekkers, and H. van de Meent, "Osseointegrated prosthesis for patients with an amputation," multidisciplinary team approach in the Netherlands Osseointegrierte Prothese fur Patienten nach Amputation. *Unfallchirurg*; vol.120: 293-299, 2017. <https://doi.org/10.1007/s00113-016-0302-1>

- [7]. R. Atallah *et al.*, “Osseointegrated transtibial implants in patients with peripheral vascular disease: a multicenter case series of 5 patients with 1-year follow up,” *J Bone Joint Surg Am*; vol.99 no. 18. pp. 1516–1523, 2017. <https://doi.org/10.2106/jbjs.16.01295>
- [8]. R. Leijendekkers *et al.*, “Longterm outcomes following lower extremity press-fit bone-anchored prosthesis surgery: a 5-year longitudinal study protocol,” *BMC Musculoskelet Disord*; vol.17, no.1, pp. 484, 2016. <https://doi.org/10.1186/s12891-016-1341-z>
- [9]. S. Jonsson, K. Caine-Winterberger, and R. Branemark, “Osseointegration amputation prostheses on the upper limbs: methods, prosthetics, and rehabilitation,” *Prosthet Orthot Int*; vol. 35, pp. 190–200, 2017. <https://doi.org/10.1177/0309364611409003>
- [10]. R. Branemark, O. Berlin, K. Hagberg, P. Bergh, B. Gunterberg, and B. Rydevik, “A novel osseointegrated percutaneous prosthetic system for the treatment of patients with transfemoral amputation,” *Bone Joint J*; vol. 96, pp. 106–113, 2014. <https://doi.org/10.1302/0301-620x.96b1.31905>
- [11]. J. Tillander, K. Hagberg, L. Hagberg, and R. Branemark, “Osseointegrated titanium implants for limb prostheses attachments: infectious complications,” *Clin Orthop Relat Res*; vol. 468, pp. 2781–2788, 2010. <https://doi.org/10.1007/s11999-010-1370-0>
- [12]. K. Hagberg, E. Haggstrom, M. Uden, and R. Branemark, “Socket versus bone-anchored trans-femoral prostheses: hip range of motion and sitting comfort,” *Prosthet Orthot Int*. vol. 29, pp. 153–163, 2005. <https://doi.org/10.1080/03093640500238014>
- [13]. A. Nebergall, C. Bragdon, A. Antonellis, J. Karrholm, R. Branemark, and H. Malchau, “Stable fixation of an osseointegrated implant system for above-the-knee amputees,” *Acta Orthop*. vol.83, pp. 121–128, 2012. <https://doi.org/10.3109/17453674.2012.678799>
- [14]. S. Abbas, and A. Kubba, “Fatigue Characteristics and Numerical Modelling Prosthetic for Chopart Amputation,” *Modelling and Simulation in Engineering* vol. 2020, <https://doi.org/10.1155/2020/4752479>
- [15]. S. Abbas, “Fatigue Characteristics and Numerical Modeling Socket for Patient with Above Knee Prosthesis,” *Defect and Diffusion Forum Journal* vol. 398, pp. 76-82, 2020. DOI: [10.4028/www.scientific.net/DDF.398.76](https://doi.org/10.4028/www.scientific.net/DDF.398.76).
- [16]. M. Al Muderis, W. Lu, K. Tetsworth, and B. Bosley, “Single-stage osseointegrated reconstruction and rehabilitation of lower limb amputees: the Osseointegration Group of Australia Accelerated Protocol-2 (OGAAP-2) for a prospective cohort study,” *BMJ Open*. vol. 7, no. 3, pp. e 013508, 2017. <https://doi.org/10.1136/bmjopen-2016-013508>
- [17]. J. Sullivan, M. Uden, K. Robinson, and S. Sooriakumaran, “Rehabilitation of the trans-femoral amputee with an osseointegrated prosthesis: the United Kingdom experience,” *Prosthet Orthot Int*. vol. 27, no.2, pp. 114-120, 2013. <https://doi.org/10.1080/03093640308726667>
- [18]. R. Branemark, O. Berlin, K. Hagberg, P. Bergh, B. Gunterberg, and B. Rydevik, “A novel osseointegrated percutaneous prosthetic system for the treatment of patients with transfemoral amputation: A prospective study of 51 patients,” *Bone Joint J*. vol.96-B, no. 1, pp. 106-113, 2014. <https://doi.org/10.1302/0301-620x.96b1.31905>
- [19]. R. Tranberg, R. Zugner, and J. Karrholm, “Improvements in hip- and pelvic motion for patients with osseointegrated trans-femoral prostheses,” *Gait Posture*. vol. 33, no. 2, pp. 165-168, 2011. <https://doi.org/10.1016/j.gaitpost.2010.11.004>
- [20]. E. Haggstrom, K. Hagberg, B. Rydevik, and R. Branemark, “Vibrotactile evaluation: osseointegrated versus socket-suspended transfemoral prostheses,” *J Rehabil Res Dev*, vol. 50, no. 10, pp. 1423-1434, 2013. <https://doi.org/10.1682/jrrd.2012.08.0135>
- [21]. H. Van de Meent, M. Hopman, and J. Frolke, “Walking ability and quality of life in subjects with transfemoral amputation: a comparison of osseointegration with socket prostheses,” *Arch Phys Med Rehabil* vol. 94, no. 11, pp. 2174-2178, 2013. <https://doi.org/10.1016/j.apmr.2013.05.020>
- [22]. D. Matthews *et al.*, “UK trial of the Osseointegrated Prosthesis for the Rehabilitation for Amputees: 1995-2018,” *Prosthet Orthot Int*, vol. 43, no.1, pp. 112-122, 2019. <https://doi.org/10.1177/0309364618791616>
- [23]. S. Kunutsor, D. Gillatt, and A. Blom, “Systematic review of the safety and efficacy of osseointegration prosthesis after limb amputation,” *Br J Surg*. vol. 105. no. 13, pp. 1731- 1741, 2018. <https://doi.org/10.1002/bjs.11005>
- [24]. M. Muderis, W. Lu, V. Glatt, and K. Tetsworth, “Two-Stage Osseointegrated Reconstruction of Posttraumatic Unilateral Transfemoral Amputees,” *Mil Med*. vol. 183(suppl-1), pp. 496-502, 2018. <https://doi.org/10.1093/milmed/usx185>
- [25]. S. Abbas, A. Takhakh, and J. Chiad, “Investigating the Future of Prosthetics Using Osseointegration Technology- Review,” *Al-Nahrain Journal for Engineering Sciences NJES* vol. 26, no. 3, pp. 186-196, 2023 <http://doi.org/10.29194/NJES.26030186NJES>.
- [26]. ASTM F1713 Standard Specification for Wrought Titanium-13Niobium-13Zirconium Alloy for Surgical Implant Applications (UNS R58130) Designation: F1713–2008 (Reapproved 2013). <https://doi.org/10.1520/fl713-08>
- [27]. ASTM D638 Type I Standard Test Method for Tensile Properties. American Society for Testing and Materials Information, Handling Series 2000 <https://doi.org/10.1520/d7812-16>
- [28]. ASTM E8/E8M – 16a Standard Test Methods for Tension Testing of Metallic Materials, American Society for Testing and Materials Information, Designation: E8/E8M – 16a. <https://doi.org/10.1520/jte20190549>
- [29]. ASTM D3479 Standard Test Method for Tension-Tension Fatigue of Polymer Matrix Composite Materials, American Society for Testing and Materials Information, Designation: D3479/D3479M – 12. https://doi.org/10.1520/d3479_d3479m-19r23
- [30]. ASTM E 9 – 89a American Society for Testing and Materials Information, Standard Test Methods of Compression Testing of Metallic Materials at Room Temperature Designation: E 9 – 89a, 2000.
- [31]. S. Abbas, A. Takhakh, J. Chiad, and B. Louhichi, “Study and Analysis of Ti13Nb13Zr Implants in the above Knee Osseointegration Prosthesis,” *Al-Qadisiyah Journal for Engineering Sciences*, vol. 17, no. 4, pp. 331–338, Dec. 2024, doi: <https://doi.org/10.30772/qjes.2024.146062.1086>